Development of Dilute Magnetic Nitride Semiconductors with Curie temperatures above 900K

N. Newman[1], Stephen Y. Wu[1], H.X. Liu[1], J. Medvedeva[2], Lin Gu[3], R.K. Singh[1], Z. G. Yu[4], I.L. Krainsky[5], S. Krishnamurthy[4], David J. Smith[3], A.J. Freeman[2], and M. van Schilfgaarde[1]

[1] *Dept. of Chemical and Materials Engin., Arizona State University, Tempe, AZ 85287-6006*
[2] *Dept. of Physics and Astronomy, Northwestern University, Evanston, IL 60208*
[3] *Dept. of Physics and Astronomy, Arizona State University, Tempe, AZ 85287-1504*
[4] *SRI International, Menlo Park, California 94025*
[5] *NASA Glenn Research Laboratory, Cleveland, Ohio 44135.*

Abstract

This article describes progress towards producing prototype magnetoelectronic structures based on III-N semiconductor materials. Our recent work on Cr-doped III-N semiconductors has explored materials' properties associated with producing, injecting, transporting, manipulating and detecting spin-polarized electron populations. Although we primarily review on our group's results on nitride semiconductors, work on other semiconductors and from other groups will also be discussed when particularly relevant.

Introduction

Spintronics is a new field aims at using both the charge and spin of an electron to realize devices that have capabilities more advanced than that of semiconductor and magnetic technologies alone [1]. Semiconductor devices used in digital electronics, analog circuits, and optoelectronics almost always utilize nearly perfect, single crystal bulk and thin film structures to produce efficient devices with small and precisely controlled dimensions. In recent years, sophisticated bandgap and interface engineering has been employed in these structures to precisely tailor the height, width and even shape of the controlling potential barriers, and to use the quantized energy of the tunneling channel for improved device performance. Magnetic devices are often used in digital storage applications involving flexible tapes and hard drives. By reducing the feature size, the density of recording media and hard drives in particular, continues to decrease markedly. Over the last few years, there has been rapid development of memory cells and sensors based on the giant magnetoresistance (GMR) of metallic multilayers and of magnetic tunnel junctions (MTJ) with ferromagnetic electrodes [2]. Both types of structures are currently been used commercially in hard-drive read-heads and work is underway to commercialize magnetic memories using MTJs.

The ability to realize all of these capabilities in a single integrated system and potentially to develop novel and more advanced functions makes dilute magnetic semiconductors (DMS) a very attractive material system for spin-based electronic applications [1]. Going beyond existing capabilities by manipulating such things as the rate of the coherent electron precession is an exciting possibility that could revolutionize information technology. Exploiting spintronics for quantum computing is one example of a potential high-impact application [3].

In order to create useful spintronic devices, we first need to understand how to produce a spin population at practical temperatures, how to inject it efficiently, how it can be propagated over useful distances, how it can be manipulated and modified and how it can be detected at a specific location. These aspects are discussed in this article. This paper is not intended to be comprehensive and we apologize in advance to those whose important work was not included in this overview.

Production of spin-polarized populations

Spin-polarized carrier populations in semiconductors were initially utilized in NEA (negative electron affinity) cesiated GaAs photocathodes [4] to produce single-spin electron packets for use in electron

accelerators. Spin-polarized electron populations were excited with circularly polarized light and the energetic electrons had to travel relatively long distances ballistically to the surface for efficient emission. It is interesting that the spin-polarized electrons are emitted through a cesiated oxide layer without significant spin-flip scattering. This is in contrast to the conclusions of the SPINs community that often report that transport through disordered interfaces causes a loss in the degree of spin polarization [4]. More recent work by Awschalom et al. used circularly polarized light to generate spin-polarized populations in a wide range of semiconductors so that the spatial diffusion and other processes can be characterized using time-resolved Faraday rotation [5,6].

Since ferromagnets have a spontaneous magnetic moment as a result of a partially or fully polarized electron spin population, it seems worthwhile to explore methods to add magnetic impurities into semiconductors to induce ferromagnetism and generate a spin-polarized population. Initially, transition-metal doped II-VI semiconductors were found to be ferromagnetic, but all had very low Curie temperatures [7]. Ferromagnetism at temperatures above 100 K in a semiconductor system was first observed in Mn-doped InAs and GaAs [8,9]. More recently, the Curie temperature of the Mn-doped GaAs system has been pushed up to over 170 K through material optimization [10]. Ferromagnetic behavior has been reported at even higher temperatures in a number of semiconducting systems including Co-doped TiO_2 [11], V-doped TiO_2 [12], Mn-doped ZnO_2 [13], Co-doped SnO_2 [14], Cr-doped AlN [15, 16, 17], Cr-doped GaN [17], and Mn-doped GaN [18]. It is still controversial whether any or all of these systems are "true" dilute magnetic semiconductors because of the possibility that a trace undetected amount of a ferromagnetic secondary phase could induce the magnetism. Our results indicate that Cr-doped III-N systems are true dilute semiconductors as we have grown high quality epitaxial thin films without any detectable secondary phases and we have shown that Cr occupying the substitutional site is responsible for the ferromagnetic properties [16,17,19]. More detailed evidence is described below. Before doing this, we describe why we chose to explore the III-N system.

1. Ferromagnetic III-nitride semiconductors would provide complementary functionality to the wide range of commercial devices already developed in this wide-gap system. These materials could be epitaxially grown and could therefore be readily integrated into existing structures.
2. The large exchange coupling in transition-metal-doped nitrides, resulting from the shorter bondlength and smaller spin-orbit coupling, was originally predicted to yield large Curie temperatures (>300K) [16,20,21].
3. The enhanced III-N growth temperatures are expected to facilitate Mn and Cr-doped growth with small levels of donor compensation, especially when compared to the As_{Ga} and I_{Mn} populations that readily occur in Mn-doped GaAs [22].
4. Nitrogen, being lighter than arsenic, has smaller spin-orbit coupling, which likely dominates spin-scattering. The III-N semiconductors are therefore likely to be an excellent choice of a host material for the transport of spin-polarized electrons over significant times and distances.
5. Bandgap engineering can be readily applied to adjust both the height and width of a barrier layer so that it might be used to inject spins, or to make device features such as resonant tunneling structures or quantum wells.
6. The III-N semiconductors are more resilient to the presence of defects. Semiconductors typically require high levels of crystalline perfection to exhibit useful electronic and optical properties. However, the performance of III-N semiconductors appears to be much less affected by the presence of extended defects than other semiconductors. Lester et al. [23] have shown that highly efficient GaN light-emitting diodes have been produced with six orders of magnitude more dislocations than GaAs diodes with similar efficiency.
7. Interface engineering is readily achieved. The interfacial potential barrier of a metal/III-N junction can be tuned from a large rectifying potential barrier to an accumulation Ohmic layer by altering the cation composition of the semiconductor and the choice of metal. For example, metal / n-GaN contacts exhibit Schottky barrier heights of ~1 eV for Au, Ni and Pt, ~0.3-0.6 eV for Cr and Ti, and ~0 for Al. In ternary alloys, the barrier height increases with increasing Al mole fraction and decreases for increasing

In mole fraction. For example, the barrier height of Ni contacts is 0.95 eV for n-GaN, 1.3 eV for n-$Al_{0.15}Ga_{0.85}N$ and 1.6 eV for n-$Al_{0.3}Ga_{0.7}N$.

While Mn has been most common dopant used to synthesize III-As and III-N magnetic semiconductors, we chose to explore Cr doping for the following reasons. Cr has a lower vapor pressure than Mn, so it would be expected to have a larger sticking coefficient at elevated growth temperatures. The limited growth temperature used during deposition of other ferromagnetic Mn-doped III-V semiconductors to overcome the high volatility of Mn is presumably responsible for the observed poor crystalline quality and high levels of compensation in these materials [22]. Since the Cr_{Al} and Cr_{Ga} t_2 defect level would be expected to be $^1/_3$ filled, the partial compensation from the commonly observed background donors that make GaN naturally n-type would be expected to drive the system towards optimal doping. Thus, this partial compensation will increase the filling in the Cr defect band from $^1/_3$ towards the optimal ½ filling for the double exchange mechanism of ferromagnetism.

GaN and AlN thin films doped with a wide range of Cr concentrations were synthesized in a custom-built UHV molecular beam epitaxy (MBE) with a typical base pressure of $<5x10^{-10}$ Torr. A tunable monoenergetic nitrogen plasma beam is supplied by an electron cyclotron resonance (ECR) source (AsTEX Model Compact). 6H-SiC (0001) and sapphire (0001) substrates were used. The thickness and depth profile of the chemical composition have been characterized by Rutherford backscattering spectroscopy (RBS) with 2.00 and 3.05 MeV He^{++} beams at incident angles of 8°. A 2.00 MeV He++ beam obtain channeling yields of Ga and Cr, and a 3.73 MeV He^{++} beam was used to obtain channeling yields of *N* by Nuclear resonant elastic scattering (NRA). Nuclear resonant elastic scattering, $^{14}N(a,a)^{14}N$ was used for *N* detection. The channeling angular distributions for Cr**,** Ga and N were obtained using a two-axis goniometer. Magnetic property measurements were carried out at low temperature (10-350K) using a superconducting quantum interference device (SQUID) magnetometer (S.H.E. VTS900) and at elevated temperature (350-1000K) using a vibrating sample magnetometer (VSM) (Quantum Design PPMS system) fitted with a high temperature oven option. All samples were measured with the magnetic field parallel to the film. X-ray diffraction was performed using a Rigaku D/MAX-IIB powder diffractometer equipped with a single crystal graphite monochromator. Measurements were made using Ti/Al contacts and a 4 point-probe technique. The microstructure of the films was characterized in the cross-sectional geometry using transmission electron microscopy (TEM) with a JEOL 4000EX high-resolution electron microscope operated at 400 keV. A detailed description of the experimental methods can be found in Ref. [16,17,19].

Figure 1(a) shows the magnetic field dependence of magnetization for 7% Cr-doped AlN at 300 and 800 K. These well defined hysteresis loops confirm that the films are ferromagnetic to temperatures well above 800K. We have observed spontaneous-magnetization values, M_s, of 18.7 emu/cm^3 at 10K and 15.4 emu/cm^3 at 300K [17]. These M_s values indicate that the effective magnetic moment in Cr-doped AlN is 0.6 μ_B/Cr atom at 10K and 0.5 μ_B/Cr atom at 300K. Since the expected magnetic moment of a Cr_{Al} defect is 3 μ_B/Cr atom, these results indicate that over 20% of the Cr atoms are magnetically active. The coercivity is 120 Oe at room temperature and 70 Oe at 800K. Figure 1(b) shows the temperature dependence on magnetization. The absence of any sudden drop in magnetization indicates a Curie temperature greater than 900K. Figure 2(a) shows the M-H curve for 2% Cr-doped GaN at 325 and 800K. The observed M_s values at 10K is 0.42 emu/cm^3, indicating that ~14% of the Cr is magnetically active. The coercive field is 100 Oe at room temperature and 60 Oe at 800K. Figure 2(b) shows the temperature dependence of magnetization up to 900K.

We have used channeling studies to conclusively show that 78%–90% of the Cr impurities occupies substitutional sites in the magnetic GaN films grown at temperatures below 775 °C, depending on the particular growth temperature [19]. Since as much as 60% of the Cr is found to be magnetically active, it is clear that the Cr_{Ga} defect plays a role in establishing the magnetic properties. Furthermore, channeling angular scans performed on these films after annealing at 825 °C show a systematic drop in the fraction of substitutional Cr and the corresponding ferromagnetic signal. This behavior establishes another direct correlation between the microscopic Cr_{Ga} defect and the magnetic properties.

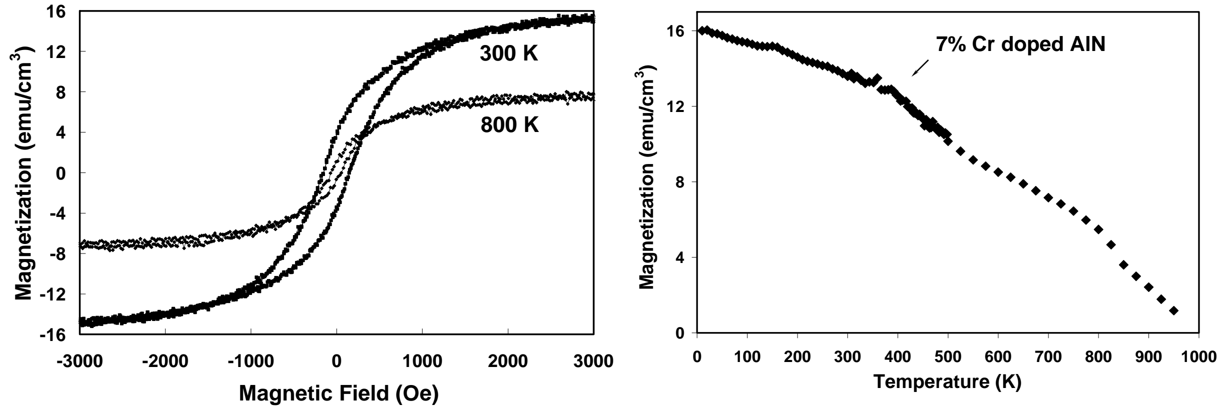

Figure 1. **(a)** Magnetic field dependence of magnetization of AlN doped with 7% Cr. **(b)** Temperature dependence of magnetization showing ferromagnetism at over 900K.

Although there has been skepticism that ferromagnetism in the Mn and Cr-doped III-Vs are partly due to secondary phases, we find no such evidence. Extensive structural characterization (TEM, EELS, XRD) confirmed that Cr-doped GaN and AlN films which are magnetic are single phase and epitaxial. TEM and XRD did not detect evidence of any ferromagnetic secondary phases. Figure 3 illustrates X-ray diffraction (XRD) data for the films. A trace amount of CrN was detected in some Cr-doped GaN films; however, CrN is known to be antiferromagnetic.

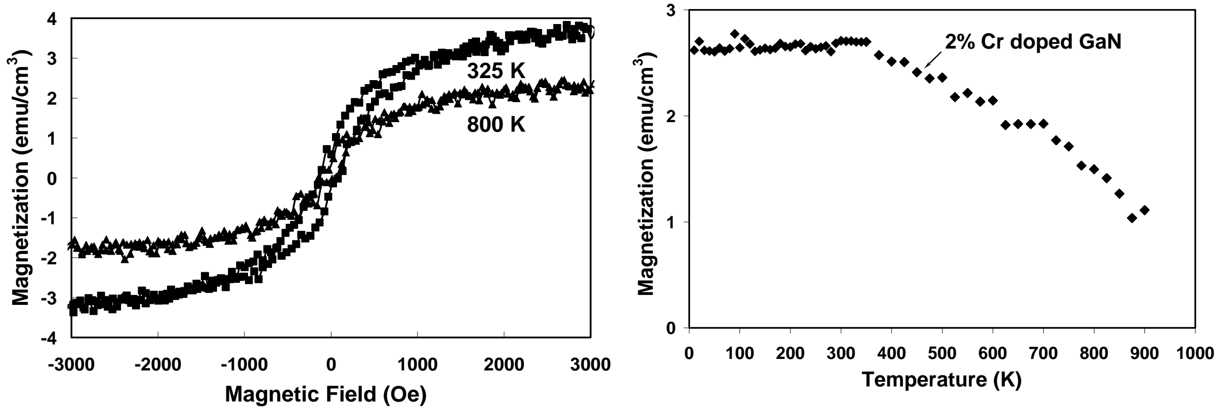

Figure 2. **(a)** Magnetic field dependence of magnetization of GaN doped with 2% Cr. **(b)** Temperature dependence of magnetization showing ferromagnetism at over 900K.

Transport

For electrical measurements, Cr-doped GaN was deposited on SiC substrates and resistivity was measured as a function of temperature. Accurate measurements could be made below 100 K since under these conditions the substrate's carriers freeze out. The thermally activated process follows the exponential law, $R=R_o\exp[(T_o/T)^{1/4}]$, characteristic of variable range hopping between localized states in an impurity band [24].

LSDA calculations find that Cr in the dilute doping limit form near midgap deep levels in both zincblende (ZB) and wurtzite (WZ) AlN [21]. The *d* level is exchange-split, and in the ZB host are further split by the crystal-field into a three-fold degenerate t_2 and a doubly degenerate *e* level, with the *e* level is ~1eV below the t_2. The majority t_2 is $^1/_3$-filled for Cr, leading to a magnetic moment of $3\mu_B$. The partial filling of the t_2 level accounts for the magnetism of substitutional Cr in GaN and AlN. Thus, we attribute the observed conduction to variable range hopping of spin-polarized electrons in the Cr impurity

band and conclude that ferromagnetism in Cr-doped GaN and AlN can be attributed to the double exchange mechanism within the partially filled Cr t_2 band.

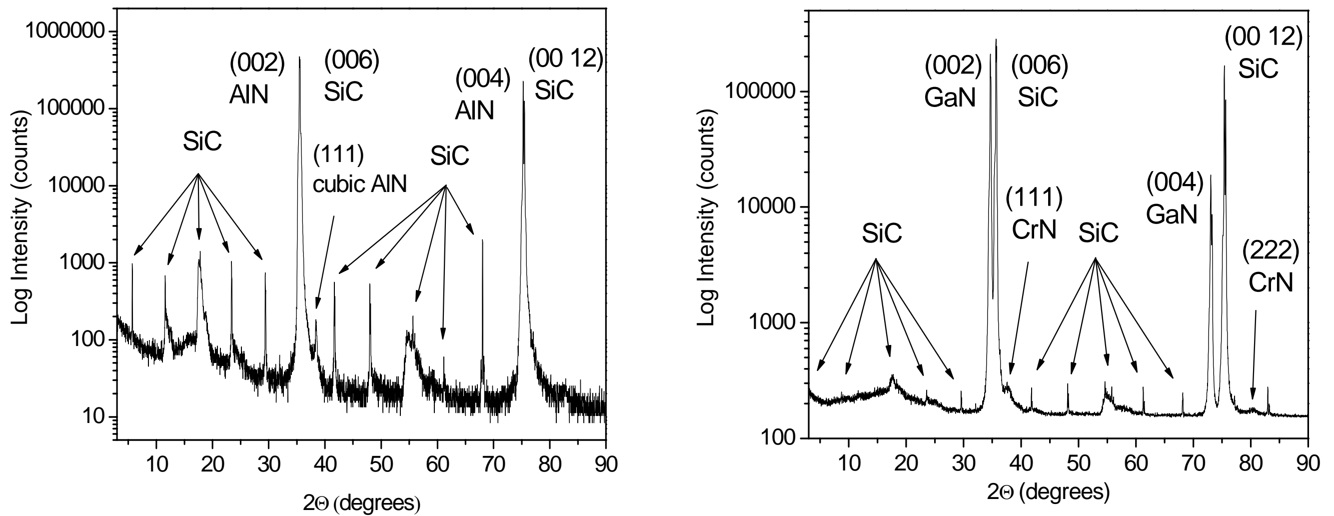

Figure 3. XRD pattern for **(a)** 7% Cr-doped AlN and **(b)** 2% Cr-doped GaN deposited on a SiC (0001) substrate.

The most interesting and useful devices might be expected to involve injection of such carriers across a tunnel barrier or heterostruture interface into the valence or conduction band of non-magnetic semiconductor region. Four very important device parameters for such systems are the spin relaxation time and the spin decay length for electrons and holes. To calculate spin relaxation time in III-N and III-As semiconductors, we have taken into account both the Elliott-Yafet and the D'yakonov-Perel' scattering mechanisms and developed an approach to treat the spin-orbit coupling accurately [25]. Unlike many previous studies, where both the spin-orbit interaction and scattering (phonons and impurities) are treated as perturbations, we include the spin-orbit interaction in the unperturbed Hamiltonian and treat scattering by ionized impurities and phonons as a perturbation. Our numerical calculations predict two orders of- magnitude longer electron spin relaxation times and an order-of magnitude shorter hole spin relaxation times in high quality samples of GaN than those in GaAs. See figure 4. The calculated electron and hole spin relaxation times in GaAs are in good agreement with experiments. [5,26-28]

We also find that realistic energy bands are required to accurately simulate the measured electron spin relaxation times, particularly for holes because simplified models usually do not adequately describe the heavily anisotropic valence bands. We find, contrary to common interpretation, that the splitting between the heavy-hole and the split-off bands at the zone center is not always an accurate measure of the spin orbit coupling strength for electrons.

Injection

Efficient injection of spin-polarized electrons has been realized across the ferromagnet/GaAs interface. In an elegant experiment, an Fe epitaxial electrode was used to inject spin-polarized electrons into a GaAs lateral device and the spin-polarized population was spatially mapped . An electron decay length of over 50 mm was measured using Kerr rotation [29]. Successful electrical injection of a spin-polarized population into a III-N structure has not been reported to date. Work in a number of labs is underway to overcome this challenge. Thus, we must turn to theory to model and predict the parameters of interest.

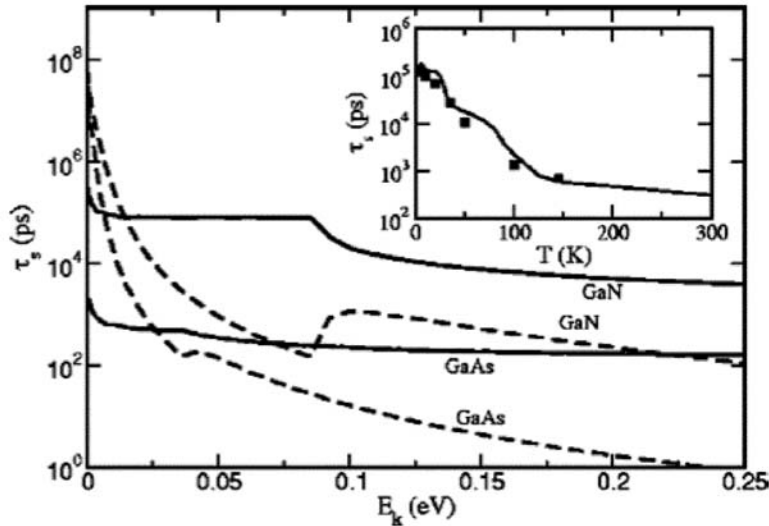

FIG. 4. Electron spin relaxation times due to the EY and DP mechanisms as a function of the electron energy in GaAs and GaN at *T*=300 K. Solid and dashed lines correspond to the contribution from the EY mechanism and the DP mechanism, respectively. The doping concentration is 10^{16} cm^{-3} and a photogenerated carrier density of $2x10^{14}$ cm^{-3} is added to the system. The inset plots the averaged spin relaxation time as a function of temperature in GaAs. Squares are experimental data reported in Ref. [5].

First-principles theoretical calculations reveal the possibility of efficient spin injection from a ferromagnetic Cr-doped GaN electrode through an AlN tunnel barrier. Cr atoms energetically prefer to segregate into the GaN region and that these interfaces retain their half-metallic behavior leading to a complete, i.e., 100%, spin polarization of the conduction electrons. This property makes the wide band-gap nitrides doped with Cr to be excellent candidates for high-efficiency magnetoelectronic devices. This is an important point as many magnetic systems, including Heusler compounds (such as NiMnSb, Co_2MnGe, Co_2CrAl) which possess the appealing half-metallic ferromagnetic behavior in bulk—show significantly reduced spin polarization at the surface [30,31] or, consequently, at the interface with a semiconductor [32]. From a comparison of the formation energy of the relaxed AlN/GaN (graded Al_xGa_xN/GaN) heterostructures with different site locations of Cr, we predict that the magnetic impurity segregates into the GaN region which serves as a ferromagnet, while AlN is the semiconductor part of the interface. Most significantly, we find that these interfaces retain the desired half-metallic behavior with a band gap in the spin minority channel of 2.7 eV, so that the conduction electrons can tunnel into the semiconductor material with 100% spin polarization. These findings mean that the wide band-gap nitride interfaces doped with Cr should make excellent candidates for applications based on spin transport.

Manipulation

Ideally, critical parameters of the spin-polarized population can be precisely manipulated. This might entail control of the degree of spin polarization or the adjustment of the precession rate. While this has been achieved in the Mn-doped GaAs system, there has not been direct evidence that this has occurred in the III-N system, at least to our knowledge.

An important mesoscopic phenomenon that involves manipulating spins of a ferromagnetic film is exchange bias. This effect uses an antiferromagnetic layer to shift the M-H hysteretic curve of a ferromagnetic layer in a magnetic tunnel junction so that one of the electrodes is pinned (hard to switch) while the other is free (easy to switch). We have made progress in realizing exchange biasing of Cr-doped GaN films using an antiferromagnetic MnO overlayer [33]. The hysteresis loop shifts laterally by 70 Oe after positive field cooling. An enhancement of the coercive field of the Cr-doped GaN film is also measured when the exchange-biasing MnO overlayer is present. The mechanism responsible for the

exchange bias is attributed to the exchange coupling at the ferromagnetic Cr–GaN/antiferromagnetic interface.

Detection

Optical measurements that monitor the Kerr rotation, Faraday rotation, and preferential circularly polarized light emission, have been used extensively in the laboratory to determine the degree of spin polarization in semiconductor structures. For the latter, a heterostructure quantum well is often used to spatially confine the injected electrons and holes so that efficient radiative recombination occurs. These methods cannot be readily applied for on-chip detection and are traditionally used for device characterization in research and development labs.

The ability to detect the spin polarization electrically is of great interest and has been realized in magnetic tunnel junctions and spin-injection resonant tunnel diodes fabricated with ferromagnetic (Ga,Mn)As electrodes and non-magnetic semiconductor barriers. [34] Successful detection of a spin-polarized population in a III-N structure by electrical means has not yet been reported to date. Work in a number of labs is underway to overcome this challenge. We have made some progress in developing a tunnel junction composed of Cr-doped GaN electrodes and an AlN tunnel barrier. Although we do see the expected parabolic conductance on voltage of a tunnel junction [35], we have not detected spin polarization.

Conclusions

Significant progress has been made towards producing, injecting, transporting, manipulating and detecting spin-polarized electron populations in III-N materials and devices. This review should provide some insight into the potential for realizing new and exciting possibilities in the area of spintronics.

Acknowledgements
The work was supported by the Defense Advanced Research Projects Agency (DARPA) and the Office of Naval Research under contracts N00014-02-1-0598, N00014-02-1-1025 and N00014-02-1-0967, the National Science Foundation under contract 0213834 and NASA under contract NAG32591.

References

1. S.A. Wolf, D.D. Awschalom, R.A. Buhrman, J.M. Daughton, S. Von Molmar, M.L. Roukes, A.Y. Chtchelkanova, and D.M. Treger, *Science* **294**, 1488 (2002); D.D. Awschalom, M.E. Flatte, and N. Samarth, Sci. Am. **286**, 52 (2002); T. Dietl, Nature Materials **2**, 646 (2003).
2. S. Parkin, X. Jiang, C. Kaiser, A. Panchula, K. Roche, and M. Samant, *Proc. of the IEEE* **91**, 661 (2003).
3. V.A. Sih, E. Johnston-Halperin, D.D. Awschalom, Proc. of the IEEE **91**, 752 (2003
4. D. T. Pierce and F. Meier, *Phys. Rev.* **B13**, 5484 (1976).
5. J.M. Kikkawa and D.D. Awschalom, Phys. Rev. Lett. **80**, 4313 (1998); J.M. Kikkawa and D.D. Awschalom, *Nature* **397**, 139 (1999).
6. B. Beschoten, E. Johnston-Halperin, D.K. Young, M. Poggio, J.E. Grimaldi, S. Keller, S.P. DenBaars, U.K. Mishra, E.L. Hu, and D.D. Awschalom,, *Phys. Rev.* **B63**, 121202 (2001).
7. M.K. Jain, Diluted magnetic semiconductors, World Scientific, River Edge, N.J., 1991.
8. H. Munekata, H. Ohno, S. von Molnar, A. Segmüller, L.L. Chang, and L. Esaki, *Phys. Rev. Lett.* **63**, 1849 (1989).
9. H. Ohno, A. Shen, and F. Matsukura, *Appl. Phys. Lett.* **69**, 363 (1996).
10. A.M. Nazmul, S. Sugahara, and M. Tanaka, *Phys. Rev.* **B67**, 241308 (2003).
11. Y. Matsumoto, M. Murakami, T. Shono, T. Hasegawa, T. Fukumora, M. Kawasaki, P. Ahmet, T. Chikyow, S. Koshihara, and H. Koinuma, *Science* **291**, 854 (2001).
12. N. H. Hong, J. Sakai, and A. Hassini, *Appl. Phys. Lett.* **84**, 2602 (2004).
13. R.K. Zheng, H. Liu, X.X. Zhang, V.A.L. Roy, and A.B. Djurišić. *Appl. Phys. Lett.* **85**, 2589 (2004).

14. S.B. Ogale, R.J. Choudhary, J.P. Buban, S.E. Lofland, S.R. Shinde, S.N. Kale, V.N. Kulkarni, J. Higgins, C. Lanci, J.R. Simpson, N.D. Browning, S. Das Sarma, H.D. Drew, R.L. Greene, and T. Venkatesan, *Phys. Rev. Lett.* **91**, 077205 (2003).
15. S.G. Yang, A.B. Pakhonmov, S.T. Hung, and C.Y. Wong, *Appl. Phys. Lett.* **81**, 2418 (2002).
16. S.Y. Wu, H.X. Liu, L. Gu, R.K. Singh, L. Budd, M. vanSchilfgaarde, M.R. McCartney, D.J. Smith, and N. Newman, *Appl. Phys. Lett.* **82**, 3047 (2003).
17. H.X. Liu, S.Y. Wu, R.K. Singh, L. Gu, D.J. Smith, N.R. Dilley, L. Montes, M.B. Simmonds, and N. Newman, *Appl. Phys. Lett.* **85**, 4076 (2004); S.Y. Wu, H.X. Liu, L. Gu, R.K. Singh, M. vanSchilfgaarde, D.J. Smith, N.R. Dilley, L. Montes, M.B. Simmonds, and N. Newman, *Mat. Res. Soc. Symp. Proc.* **Y 10.57**, 798 (2004).
18. F.E. Arkun, M.J. Reed, E.A. Berkman, N.A. El-Masry, J.M. Zavada, M.L. Reed, and S.M. Bedair, *Appl. Phys. Lett.* **85**, 3809 (2004).
19. R.K. Singh, S.Y. Wu, H.X. Liu, L. Gu, D.J. Smith, and N. Newman, *Appl. Phys. Lett.* **86**, 012504 (2005).
20. T. Dietl, H. Ohno, F. Matsukura, J. Cibert, and D. Ferrand, *Science* **287**, 1019 (2000).
21. M. van Schilfgaarde and O.N. Mryasov, *Phys. Rev.* **B63**, 233205 (2001).
22. K.M. Yu, W. Walukiewicz, T. Woitowicz, I. Kuryliszyn, X. Liu, Y. Sasaki and J.K. Furdyna, *Phys. Rev.* **B65**, 201303 (2002).
23. S.D. Lester, F.A. Ponce, M.G. Craford, and D.A. Steigerwald, *Appl. Phys. Lett.* **72**, 2562 (1998).
24. N.F. Mott, Proc. Cambridge Philos. Soc. **32**, 281 (1949).
25. Z.G. Yu, S. Krishnamurthy, M. van Schilfgaarde and N. Newman, *Phys. Rev.* **B71**, 245312 (2005).
26. J. Hilton and C. L. Tang, Phys. Rev. Lett. **89**, 146601 (2002).
27. Y. Yafet, in Solid State Physics, edited by F. Seitz and D. Turnball, Academic, New York, 1963, Vol. 14.
28. G. E. Pikus and A. N. Titkov, Optical Orientation. North Holland, Amsterdam, 1983.
29. S.A.Crooker, M. Furis, X. Lou, C. Adelmann, D.L.Smith, C.J. Palmstrom and P.A. Crowell, *Science* **309**, 2191 (2005).
30. R.J. Soulen Jr., J.M. Byers, M.S. Osofsky, B. Nadgorny, R. Ambrose, S.F. Cheng, P.R. Broussard, C.T. Tanaka, J. Nowak, J.S. Moodera, A. Barry, and J.M.D. Coey, *Science* **282**, 85 (1998); C.T. Tanaka, J. Nowak, and J.S. Moodera, *J. Appl. Phys.* **86**, 6239 (1999).
31. D. Ristoiu, J.P. Nozières, C.N. Borca, T. Komesu, H.-K. Jeong, and P.A. Dowben, *Europhys. Lett.* **49**, 624 (2000).
32. G. A. de Wijs and R. A. de Groot, Phys. Rev. B **64**, 020402(R) (2001); S. Picozzi, A. Continenza, and A. J. Freeman, *J. Appl. Phys.* **94**, 4723 (2003); A. Debernardi, M. Peressi, and A. Baldereschi, *Mater. Sci. Eng.* **C23**, 743 (2003); I. Galanakis, cond-mat, 0408204.
33. H.X. Liu, S.Y. Wu, R. Singh, and N. Newman, *J. Appl. Phys.* **98**, 046106 (2005).
34. H. Ohno, *Science* **281**, 951 (1998); D. Chiba, F. Matsukura, and H. Ohno, Physica E **21**, 966 (2004).
35. J.M. Rowell, Tunneling Phenomena in Solid, edited by E. Burstein and S. Lundqvist (Plenum, New York, 1969), p.385.